

PSR Report 2168
Revised 24 May 1991

CHOICE OF INFRARED WAVEBAND FOR A DUAL SPECTRUM (VISIBLE/INFRARED) IMAGING LINE SCANNER

P. M. Moser
C. S. Kaufman
M. Hryszko

April 1991

Interim Report
Contract N00019-90-C-0276

Sponsored by
Naval Air Systems Command
Code AIR-5471D
Washington, DC 20361-5470



PACIFIC-SIERRA RESEARCH CORPORATION
12340 Santa Monica Boulevard • Los Angeles, California 90025 • (213) 820-2200

| REPORT DOCUMENTATION PAGE | | | Form Approved OMB No. 0704-0188 | |
|--|---|--|--|--|
| Public reporting burden for this collection of information is estimated to average 1 hour per response, including the time for reviewing instructions, searching existing data sources, gathering and maintaining the data needed, and completing and reviewing the collection of information. Send comments regarding this burden estimate or any other aspect of this collection of information, including suggestions for reducing this burden, to Washington Headquarters Services, Directorate for Information Operations and Reports, 1215 Jefferson Davis Highway, Suite 1204, Arlington, VA 22202-4302, and to the Office of Management and Budget, Paperwork Reduction Project (0704-0188), Washington, DC 20503. | | | | |
| 1. AGENCY USE ONLY (Leave blank) | | 2. REPORT DATE April 1991 | | 3. REPORT TYPE AND DATES COVERED Interim Report |
| 4. TITLE AND SUBTITLE CHOICE OF INFRARED WAVEBAND FOR A DUAL SPECTRUM (VISIBLE/INFRARED) IMAGING LINE SCANNER | | | 5. FUNDING NUMBERS N00019-90-C-0276 | |
| 6. AUTHOR(S) P. M. Moser C. S. Kaufman M. Hryszko | | | | |
| 7. PERFORMING ORGANIZATION NAME(S) AND ADDRESS(ES) Pacific-Sierra Research Corporation 12340 Santa Monica Boulevard Los Angeles, CA 90025 | | | 8. PERFORMING ORGANIZATION REPORT NUMBER Report 2168 | |
| 9. SPONSORING/MONITORING AGENCY NAME(S) AND ADDRESS(ES) Naval Air Systems Command Code AIR-5471D Washington, DC 20361-5470 | | | 10. SPONSORING/MONITORING AGENCY REPORT NUMBER | |
| 11. SUPPLEMENTARY NOTES | | | | |
| 12a. DISTRIBUTION/AVAILABILITY STATEMENT Distribution unlimited | | | 12b. DISTRIBUTION CODE | |
| 13. ABSTRACT (Maximum 200 words) This report documents the results of a study to determine the optimum infrared (IR) band over which to operate for a common aperture configuration a dual band (EO/IR) imaging line scanner for airborne tactical operations. Performance requirements include wide-angle, real-time, remotely viewable, registrable (fusible), and simultaneous visible and IR imagery. The sensor must have a lateral field of view of 120 to 160 deg and be capable of operating at aircraft speeds up to 600 kn and altitudes as low as 200 ft. Factors considered in the analysis included the spectral distribution of radiation from scenes of interest, spectral atmospheric transmission, spectral detectivity of available detectors, climate considerations, effects of diffraction on resolution, availability of optical materials, detector cooling, complementarity of imaged target information, and effects of atmospheric aerosols. It was concluded that the long wavelength IR band (nominally 8 to 13 μm) would be optimum. | | | | |
| 14. SUBJECT TERMS Infrared line scanner Dual band sensor Multispectral sensor | | | 15. NUMBER OF PAGES 29 | |
| EO/IR real-time surveillance sensor Common aperture multispectral sensor Reconnaissance sensor | | | 16. PRICE CODE | |
| 17. SECURITY CLASSIFICATION OF REPORT UNCLASSIFIED | 18. SECURITY CLASSIFICATION OF THIS PAGE UNCLASSIFIED | 19. SECURITY CLASSIFICATION OF ABSTRACT UNCLASSIFIED | 20. LIMITATION OF ABSTRACT UL | |

PREFACE

This report describes the results of a study which was undertaken to determine the optimum infrared (IR) waveband of operation for a dual band (EO/IR) airborne common aperture reconnaissance sensor. The study is part of a larger task to develop a design concept for a next-generation common aperture multispectral sensor (CAMS) for the Reconnaissance and Imaging Systems Division of the Naval Air Systems Command, AIR-547; contract no. N00019-90-C-0276.

SUMMARY

Candidate infrared (IR) wavebands of operation for airborne imaging reconnaissance systems are the mid-wavelength IR band (MWIR--nominally 3.0 to 5.3 μm) and the long-wavelength IR band (LWIR--nominally 8 to 13 μm). Factors considered in selecting the optimum IR band for a common aperture, dual band (visible and IR) imaging sensor included the spectral distribution of radiation from scenes of interest, spectral atmospheric transmission, spectral detectivity of available detectors, climate considerations, effects of diffraction on resolution, availability of optical materials, detector cooling, complementarity of imaged target information, and effects of atmospheric aerosols. It was concluded that the LWIR band would be optimum.

CONTENTS

| | |
|--|-----|
| PREFACE | iii |
| SUMMARY | v |
| FIGURES | ix |
| Section | |
| 1. INTRODUCTION | 1 |
| 2. TECHNICAL DISCUSSION | 2 |
| Design performance trade-off equation | 2 |
| Radiation laws | 3 |
| Atmospheric transmission | 4 |
| Thermal derivative of Planck's radiation equation | 4 |
| Radiance contrast | 4 |
| Combination of thermal derivative and atmospheric transmission | 10 |
| Spectral detectivity | 10 |
| Joint effects of spectral atmospheric transmission and spectral detectivity | 15 |
| Climate considerations | 15 |
| Effects of diffraction on resolution | 17 |
| Optical materials | 17 |
| Detector cooling | 23 |
| Spectral band limits | 24 |
| Complementarity versus redundancy of imaged target information | 25 |
| Imaging through aerosol distributions | 27 |
| 3. CONCLUSIONS | 28 |
| REFERENCES | 29 |

FIGURES

| | |
|--|----|
| 1. Spectral radiant emittance of a blackbody at temperatures of 283, 288, and 293 K | 5 |
| 2. Transmittance of U.S. Standard Atmosphere for 1-nmi path length, 23-km visibility, and 17 mm of precipitable water in path calculated by LOWTRAN 7 | 6 |
| 3. Apparent spectral radiant emittance of a blackbody viewed through a representative atmospheric path | 7 |
| 4. Thermal derivative of spectral radiant emittance for a 288-K blackbody | 8 |
| 5. Contrast in spectral radiant emittance per degree difference in temperature of a 288-K blackbody radiator | 9 |
| 6. Product of the thermal derivative of spectral radiant emittance and atmospheric transmittance | 11 |
| 7. Cumulative integrals of the product of the thermal derivative of spectral radiant emittance and atmospheric transmittance in the 3- to 5.5- μm and 8- to 12.5- μm bands | 12 |
| 8. Spectral detectivities of selected above-average IR detectors | 13 |
| 9. Spectral detectivities of selected IR detectors weighted by the thermal derivative of spectral radiance of a 288-K blackbody | 14 |
| 10. Spectral detectivities of selected IR detectors weighted by the thermal derivative of spectral radiance of a 288-K blackbody and the spectral transmittance of a selected atmospheric path | 16 |
| 11. Contributions to the MTF of the ATARS IRLS | 18 |
| 12. Transmission bands of common optical materials | 20 |
| 13. Optical transmission of zinc sulfide | 21 |
| 14. Reflectivities of common metallic coatings | 22 |
| 15. Comparison of reflected and emitted radiation from a graybody | 26 |

SECTION 1 INTRODUCTION

Under Contract no. N00019-90-C-0276 with the Naval Air Systems Command (NAVAIR), Pacific-Sierra Research Corporation (PSR) is pursuing Phase I of a Small Business Innovation Research (SBIR) project entitled "Multispectral Electro-Optical/Infrared Real-Time Sensor." The ultimate objective of the SBIR project (Topic Description N90-101) is to design an airborne real-time sensor capable of producing indexed imagery in both the visible and infrared (IR) bands. The sensor would have a lateral field of view (FOV) of 120 to 160 deg and be capable of operating at aircraft speeds up to 600 kn and altitudes as low as 200 ft.

At a meeting of NAVAIR, Naval Air Test Center, Synectics Corporation, Control Data Corporation (CDC), and PSR representatives on 16 January 1991, it was agreed that PSR would be concerned with the "front end" of an imaging system that would provide wide-angle, real-time, remotely viewable, registrable (fusible) imagery simultaneously in both the visible and IR bands, while Synectics and CDC would be concerned with processing, storing, transmitting, and reconstituting the resulting data.

More specifically, the objective of the overall multiphase SBIR project is to provide, with a single equipment but with no reduction in performance, the capabilities of the low altitude electro-optical imager and the IR line scanner (IRLS) that are currently subsystems within the Advanced Tactical Air Reconnaissance System (ATARS).

It was agreed at the meeting of 16 January 1991 to regard the AN/AAD-5 IRLS as the archetype equipment and to investigate the possibility of modifying it to operate in two spectral bands.

An issue remaining to be decided was the particular IR band to be selected: the mid-wavelength IR band (MWIR--nominally 3.0 to 5.3 μm) or the long-wavelength IR band (LWIR--nominally 8 to 13 μm). The purpose of this report is to investigate and resolve that issue.

SECTION 2

TECHNICAL DISCUSSION

DESIGN-PERFORMANCE TRADE-OFF EQUATION

A number of factors govern the selection of the spectral band in which a passive IR imaging device is designed to operate. These include the spectral distribution of radiant power emitted and reflected from the targets and backgrounds of interest, the variation of such radiant power as a function of target/scene temperature, the ratio of this variation of radiation to the total power radiated, the relative transparency of the atmosphere, diffraction effects, and the cost and availability of suitable optical materials, IR detectors, and cryostats.

To a first approximation, the performance of a scanning passive IR imaging device can be related to its design parameters by the equation [Moser and MacMeekin, 1973]

$$\frac{(\Omega F)^{\frac{1}{2}}}{\omega \Delta T} = \frac{D}{4 f / n o} (2 n E_s)^{\frac{1}{2}} \int_{\lambda_1}^{\lambda_2} D^*(\lambda) E_o(\lambda) M'(\lambda) \tau_a(\lambda) d\lambda \quad (1)$$

where Ω = total solid angle scanned by all the detectors per frame (sr)

F = scanner frame rate (s^{-1})

ω = instantaneous solid angle resolution (sr) of a single detector projected through the optical system

ΔT = temperature difference in an extended blackbody at the target location that yields a unity signal-to-noise ratio (K)

$D^*(\lambda)$ = spectral detectivity of an IR detector over the wavelength range of interest ($cm \cdot Hz^{1/2}/W$)

D = effective aperture diameter of the collecting optics (cm)

n = number of active IR detectors in the scanning array (dimensionless)

f/no = ratio of effective focal length and effective aperture diameter (dimensionless)

E_s = scanning efficiency (dimensionless)

$E_o(\lambda)$ = optical efficiency over the wavelength range of interest (dimensionless)

$M'(\lambda)$ = thermal derivative of target spectral radiant emittance over the wavelength range of interest ($W \cdot cm^{-2} \cdot K^{-1}$)

λ_1 = IR band cut-on wavelength

λ_2 = IR band cut-off wavelength

$\tau_a(\lambda)$ = spectral transmittance of the atmosphere over the path and wavelength range of interest.

The left side of Eq. (1), sometimes called the "index of performance" of the equipment, is a composite of the performance parameters of sensitivity, resolution, FOV, and frame/line rate. The right side of the equation is a composite of design parameters. It can be seen from the wavelength-dependent factors in Eq. (1), that the choice of spectral band (as far as thermal sensitivity is concerned) is governed by the following parameters: the thermal derivative of target spectral radiant emittance, the spectral transmittance of the atmosphere, the spectral detectivity of the detector material, and the optical efficiency, which includes the spectral transmittances of the optical materials.

RADIATION LAWS

Most objects in a terrestrial scene emit radiation over a broad range of wavelengths at rates that are proportional to both the fourth power of their absolute temperatures and to their radiant efficiencies (emissivities). The wavelength λ_m at which this radiation has its peak value varies inversely as the absolute temperature and is given by Wien's displacement law

$$\lambda_m = \frac{2898 (\mu\text{m} \cdot \text{K})}{T (\text{K})} \quad (2)$$

Thus, radiation emitted by an object at room temperature (nominally $72^\circ\text{F} = 22^\circ\text{C} = 295 \text{ K}$) peaks at a wavelength of $9.8 \mu\text{m}$ while radiation emitted from the interior of the exhaust nozzle of a jet engine of temperature 500°C (773 K) peaks at a wavelength of $3.7 \mu\text{m}$. Accordingly, the first consideration in the choice of an optimum spectral band would appear to be the range of temperatures expected in targets of interest. However, for IR imaging devices, such as an IR line scanner (IRLS) or a forward-looking IR (FLIR) imaging device, it is generally not sufficient simply to detect a target but to produce an interpretable image in the context of its background. Even if a target is significantly hotter than its background, and thus easily detectable at the shorter wavelengths, sensitivity at the longer wavelengths is still generally necessary to image the cool background as well.

Blackbody objects (emissivity = 1) emit radiation as a function of wavelength in accordance with the Planck radiation law. Figure 1 shows plots of the Planck function for three temperatures.

ATMOSPHERIC TRANSMISSION

Atmospheric transmission "windows" exist over wavelength intervals of roughly 3 to 5.3 μm (mid-IR) and 7.5 to 13 μm (far-IR) as shown in Fig. 2. If one multiplies the 15°C (288 K) spectral radiance curve of Fig. 1 by the transmittance curve of Fig. 2, one obtains the curve of Fig. 3 which provides a meaningful indication of the spectral distribution of radiant power available over a representative path for the situation in which one is interested primarily in observing emissivity variations (i.e., temperature is not the significant variable) in the scene.

THERMAL DERIVATIVE OF PLANCK'S RADIATION EQUATION

On the other hand, if one is interested primarily in temperature variations in the scene, then the first partial derivative of the spectral radiance with respect to temperature, which is plotted in Fig. 4, is a more meaningful variable. In the absence of atmospheric transmission losses, this curve peaks at a wavelength of about 8.5 μm for a 15°C blackbody/graybody.

RADIANCE CONTRAST

In certain situations, e.g., in which the total radiation, rather than variations in it, is detected and processed, dynamic range may become a wavelength-dependent problem. (An example of such a situation might be a staring-array imaging system.) To illustrate, if one divides the temperature derivative of the spectral radiant emittance (Fig. 4) by the spectral radiant emittance for a 288-K blackbody (Fig. 1), one obtains a spectral radiant emittance contrast curve (Fig. 5) which shows that the radiance contrast in the far-IR range is only about 1.7 percent per kelvin whereas in the mid-IR interval, the radiance contrast is about 4.3 percent per kelvin. Accordingly, imaging of small temperature variations with a staring-array system may be more difficult in the long wavelength IR band than in the mid-wavelength band because contrasts against a relatively large background are only about 40 percent as great.

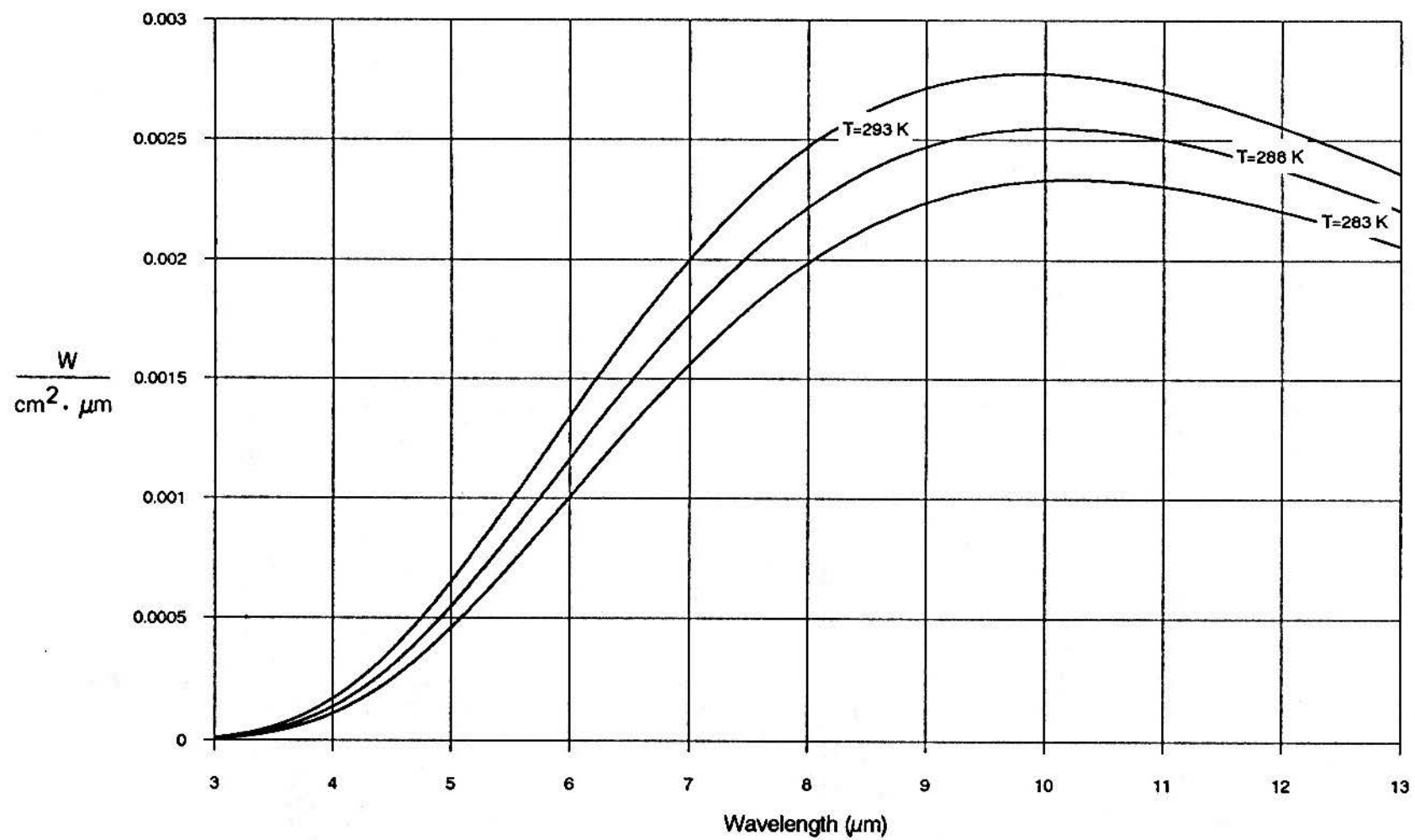


Figure 1. Spectral radiant emittance of a blackbody at temperatures of 283, 288, and 293 K.

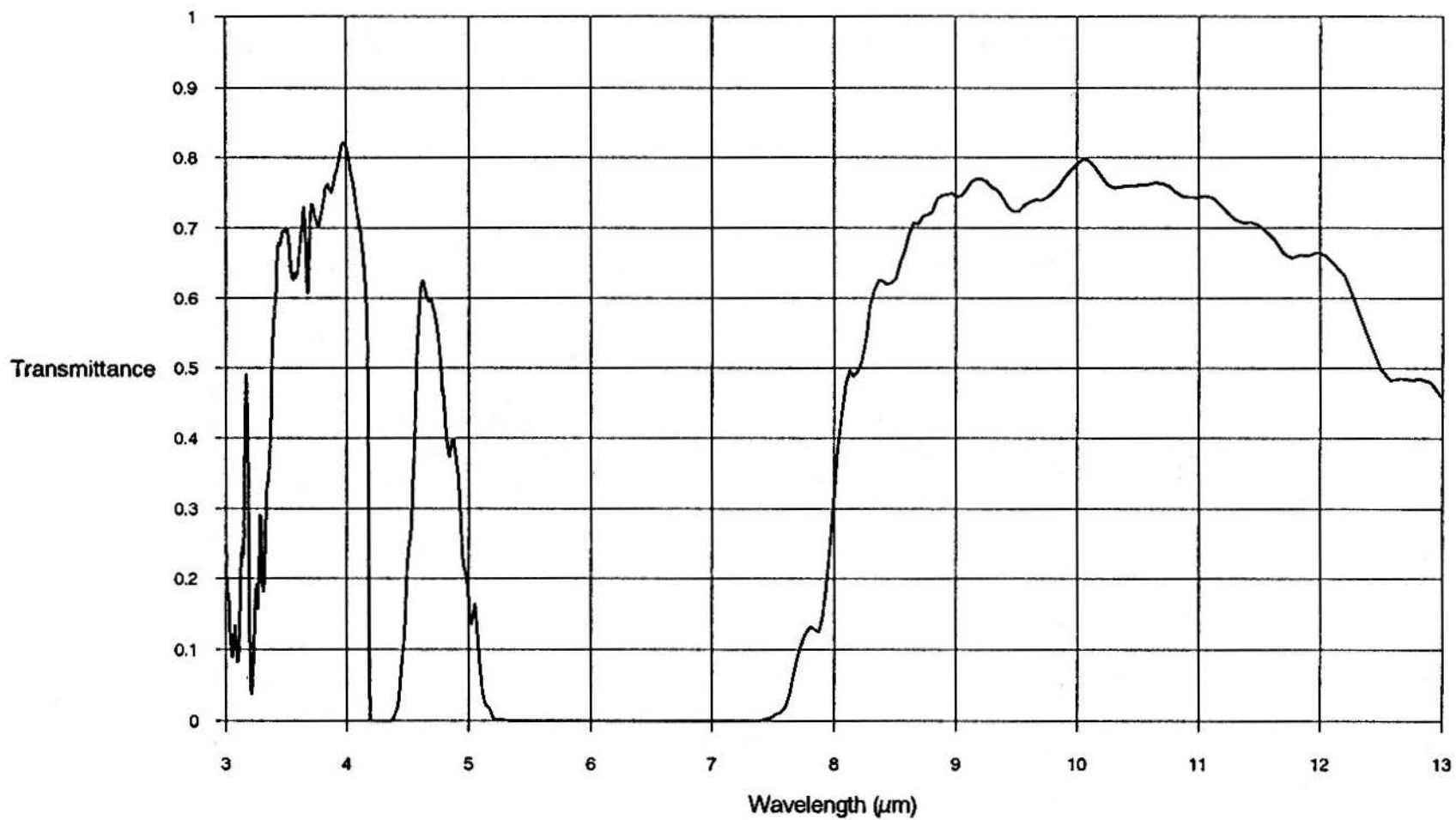


Figure 2. Transmittance of U.S. Standard Atmosphere for 1-nmi path length, 23-km visibility, and 17 mm of precipitable water in path calculated by LOWTRAN 7.

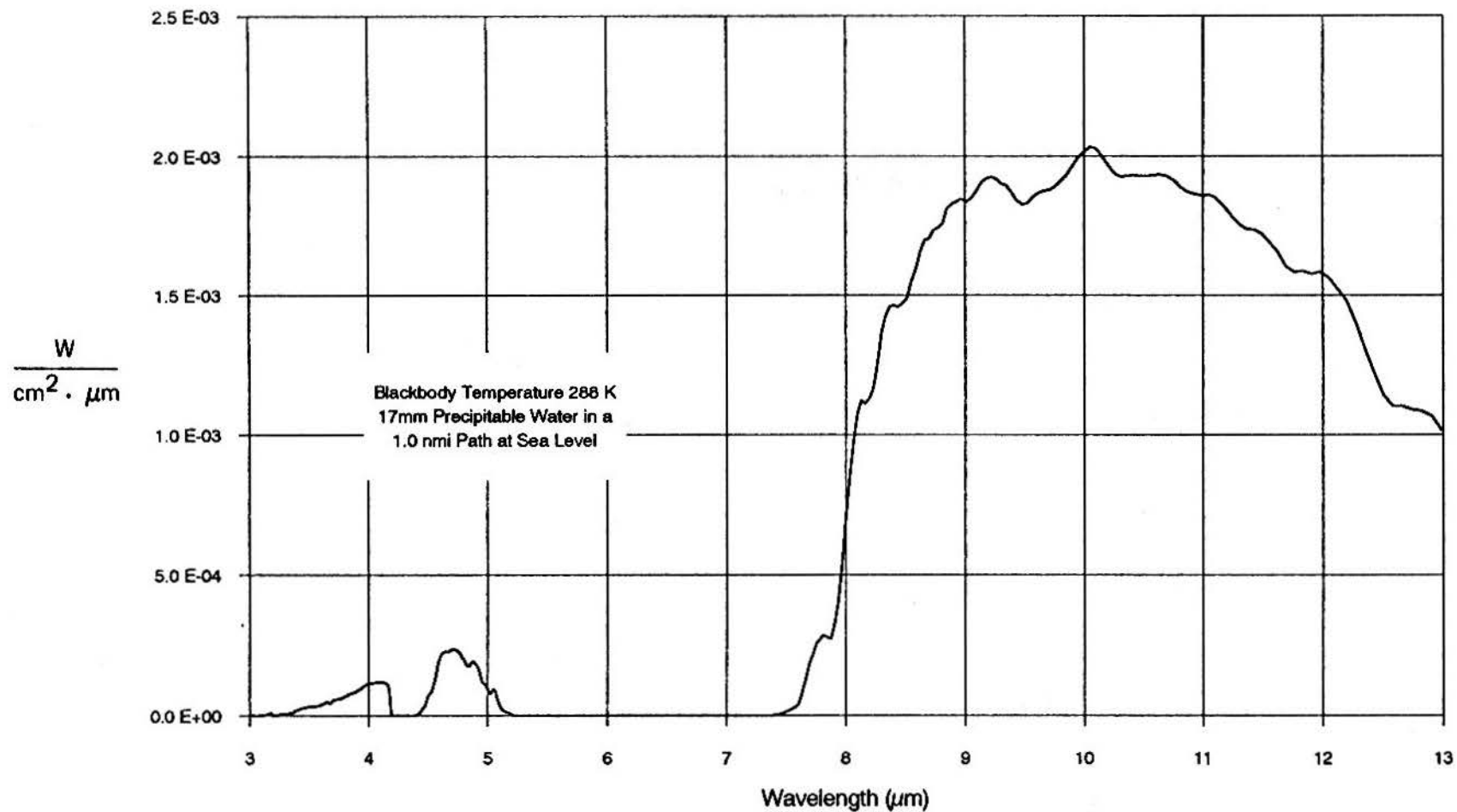


Figure 3. Apparent spectral radiant emittance of a blackbody viewed through a representative atmospheric path.

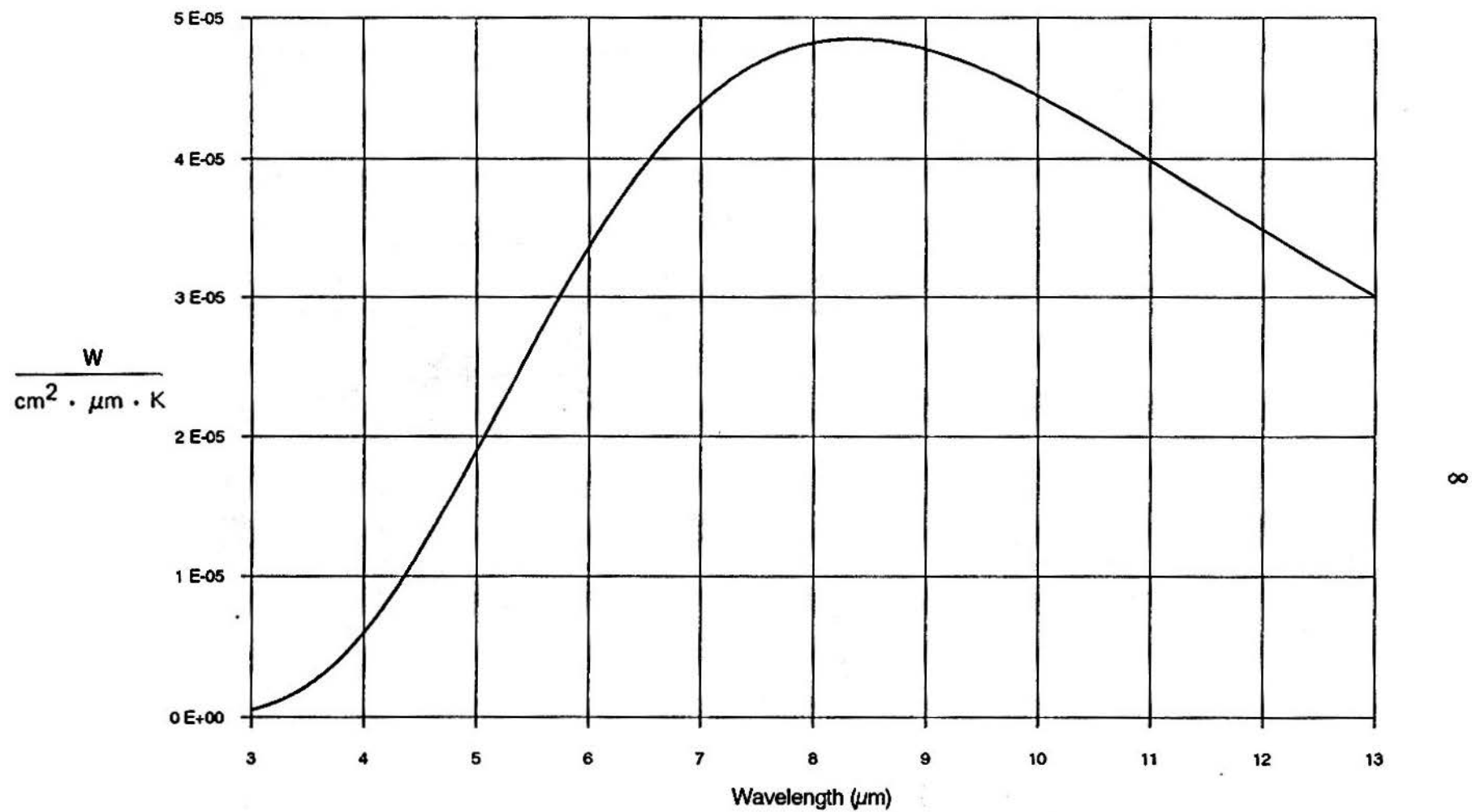


Figure 4. Thermal derivative of spectral radiant emittance for a 288-K blackbody.

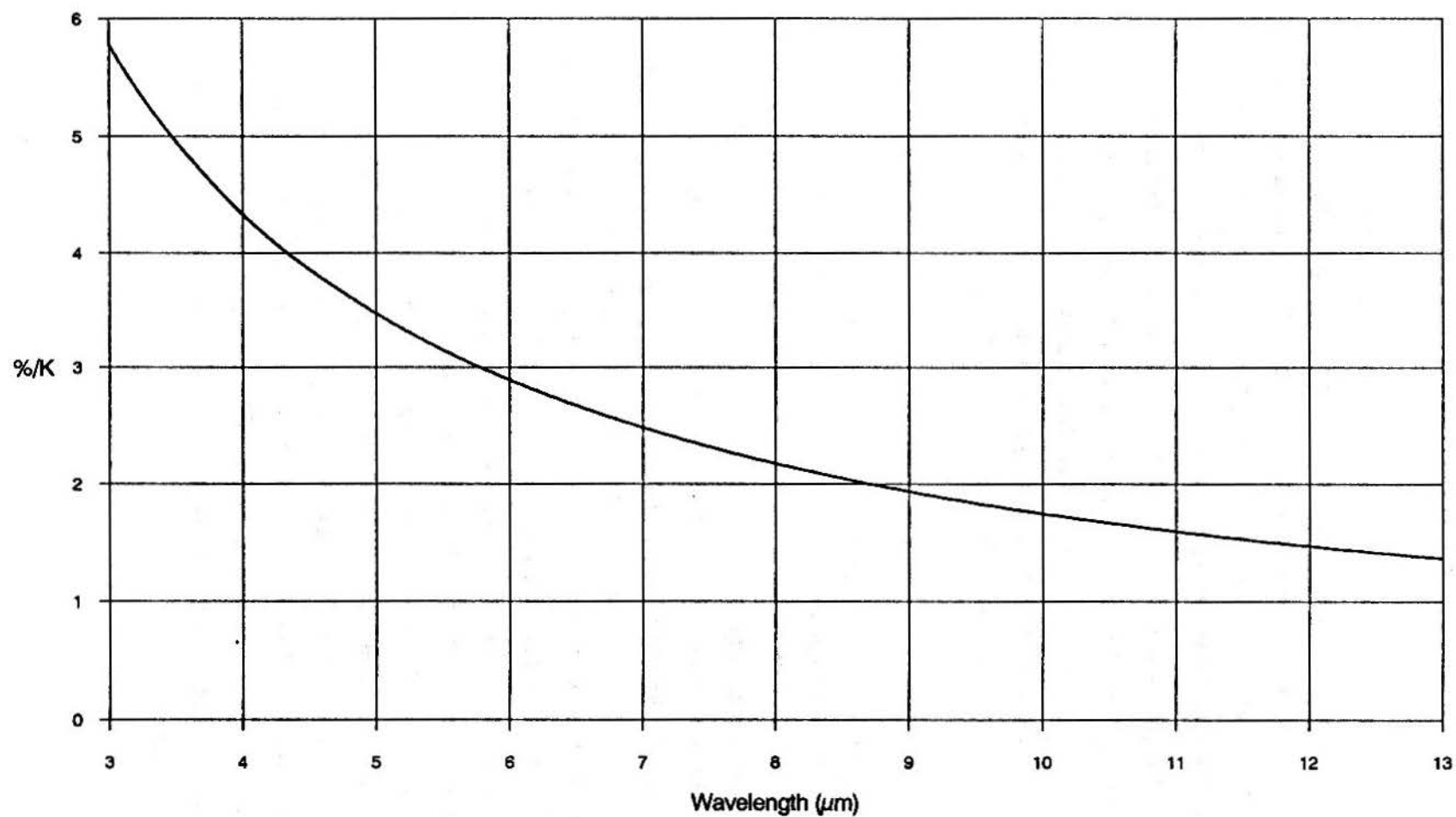


Figure 5. Contrast in spectral radiant emittance per degree difference in temperature of a 288-K blackbody radiator.

COMBINATION OF THERMAL DERIVATIVE AND ATMOSPHERIC TRANSMISSION

If one is interested in determining the effect of atmospheric attenuation on an imaged thermal scene, one can multiply the temperature derivative of the spectral radiance curve (Fig. 4) by the atmospheric transmittance curve (Fig. 2) to determine the spectral distribution of the effective variation of radiant power, to which the detected signals will be proportional as shown in Fig. 6. Numerical integration of the three portions of the curve of Fig. 6 reveals that $130 \mu\text{W}/\text{cm}^2/\text{K}$ is available in the far-IR interval whereas only $6.2 \mu\text{W}/\text{cm}^2/\text{K}$ is available over the mid-IR interval---a factor of 21 difference (see Fig. 7). As can be seen in Eq. (1), this disadvantage could be overcome by increasing the diameter of the optical system, by increasing the number of detectors in the array, and/or by utilizing a detector of higher detectivity.

SPECTRAL DETECTIVITY

The spectral detectivity D^* of a particular detector is a function, among other things, of its composition, temperature, and operating wavelength. Figure 8 shows representative spectral detectivities of two quantum detector types commonly used today. Indium antimonide exhibits excellent sensitivity in the mid-IR band. Mercury cadmium telluride may be thought of as an alloy of mercury telluride and cadmium telluride; the spectral response of this detector material can be controlled in manufacture by adjusting the relative amounts of these two compounds in the alloy. A composition consisting of 80 percent HgTe and 20 percent CdTe provides peak detectivity at a wavelength of about $10 \mu\text{m}$ as shown in Fig. 8. Note that the peak detectivity of InSb at $5.2 \mu\text{m}$ is about five times greater than that of HgCdTe at $10 \mu\text{m}$. This characteristic can be used to compensate to a certain extent for the 21-fold energy disadvantage suffered by the mid-IR waveband discussed above. Figure 9, which was obtained by multiplying the curves of Fig. 8 by that of Fig. 4, illustrates how the two detectors compare in the absence of atmospheric transmission losses when they view small temperature differences in a 288-K blackbody. By numerical integration of the area under each curve, it is found that the signal-to-noise ratio (SNR) achieved with the HgCdTe detector is about twice the value for the InSb detector. Thus, for this situation, the HgCdTe detector enjoys a 2 to 1 advantage over the InSb detector.

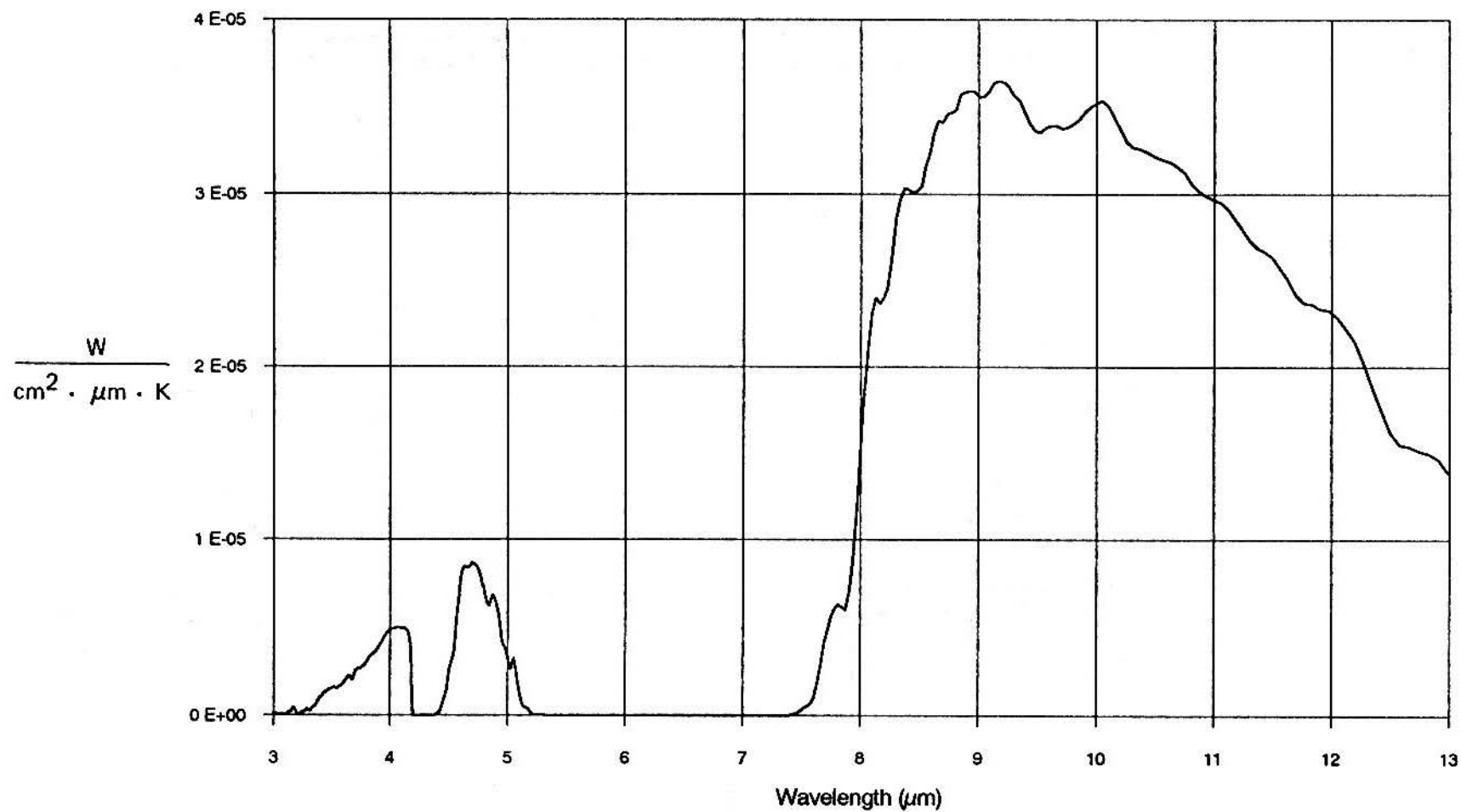


Figure 6. Product of the thermal derivative of spectral radiant emittance and atmospheric transmittance.

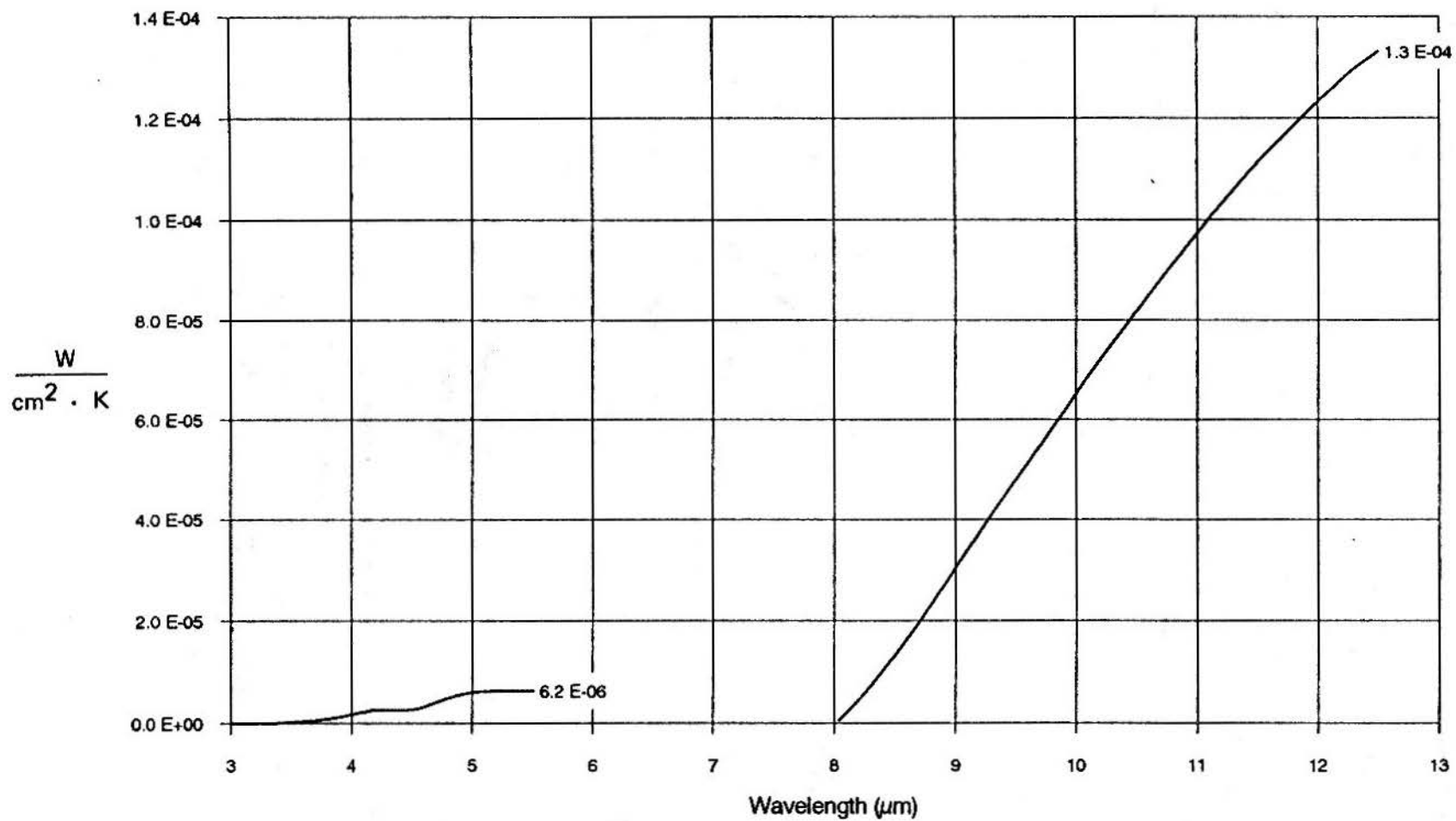


Figure 7. Cumulative integrals of the product of thermal derivative of spectral radiant emittance and atmospheric transmittance in the 3- to 5.5- μm and 8- to 12.5- μm bands.

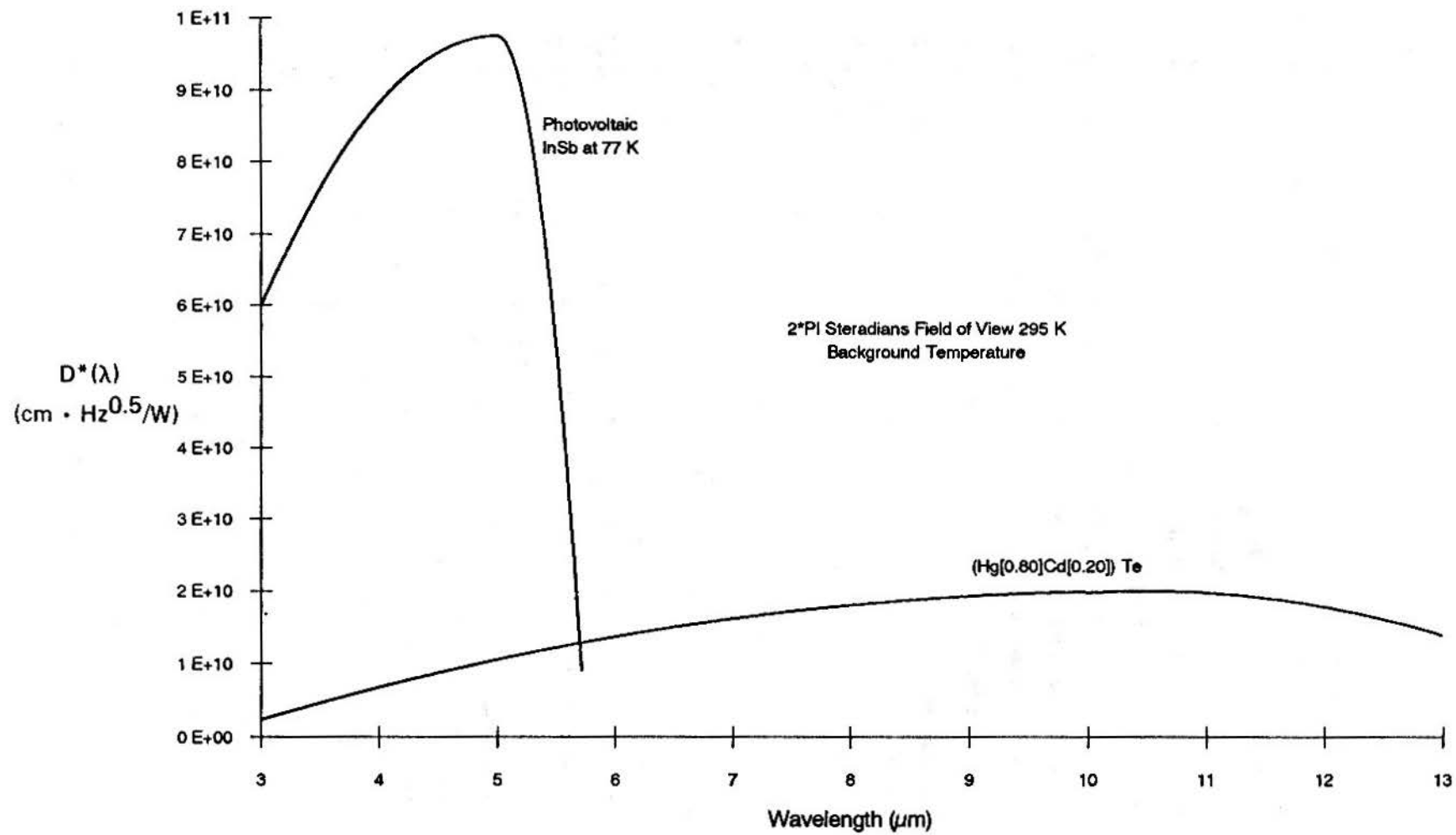


Figure 8. Spectral detectivities of selected above-average IR detectors.

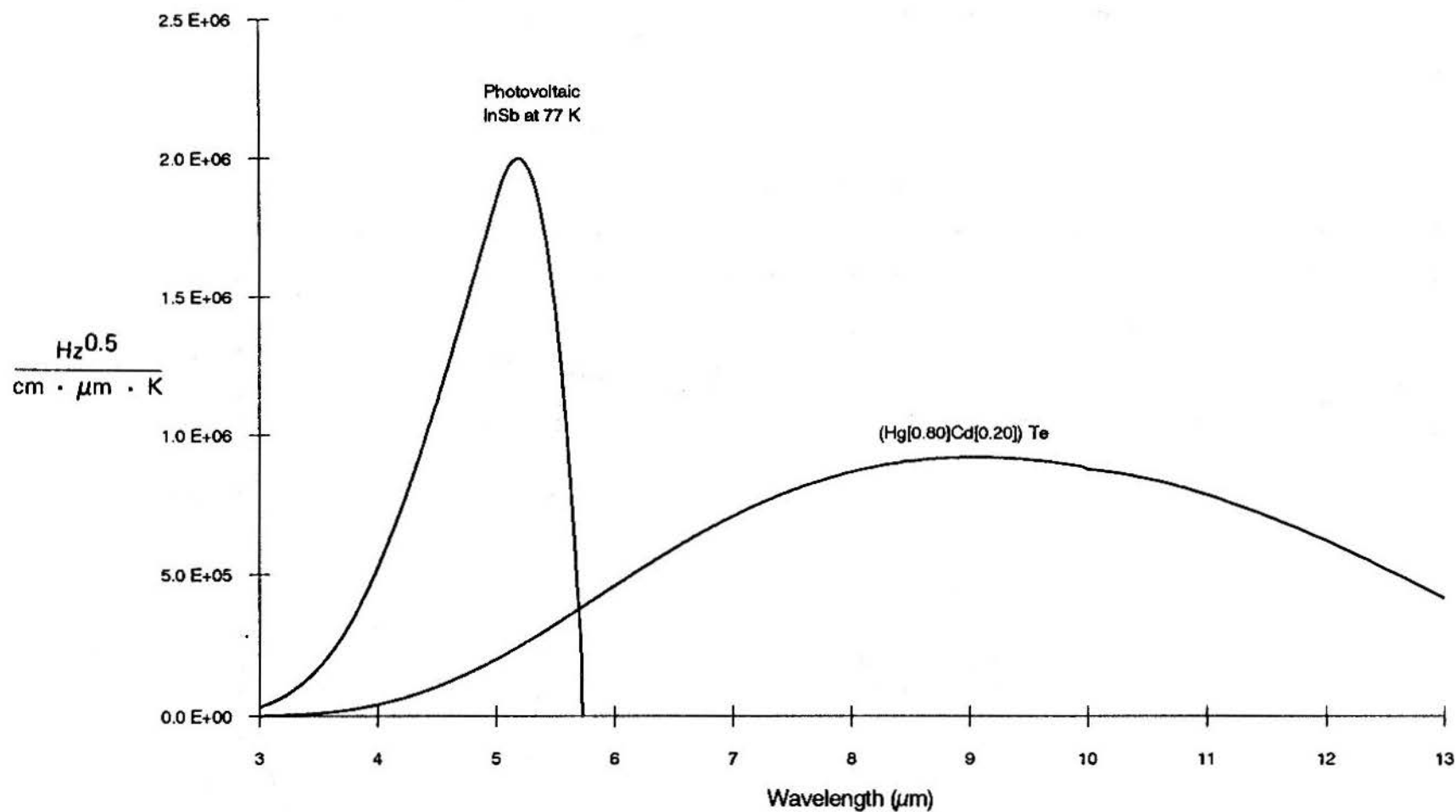


Figure 9. Spectral detectivities of selected IR detectors weighted by the thermal derivative of spectral radiancy of a 288-K blackbody.

JOINT EFFECTS OF SPECTRAL ATMOSPHERIC TRANSMISSION AND SPECTRAL DETECTIVITY

Next, consider the effects of atmospheric transmission losses on the two bands. If the curve of Fig. 6 is multiplied by those of Fig. 8, the curves of Fig. 10 are obtained. Note that HgCdTe responds weakly in the 3.0- to 5.3- μm band in addition to the 8- to 13- μm band. In practice, however, a filter is generally inserted in front of the detector to eliminate wavelengths shorter than about 8.0 μm to reduce the radiation received from the atmosphere, which contributes noise but no signal. Figure 10 shows a poorer-than-might-have-been-expected response for the indium antimonide detector because the wavelength at which the detector's response peaks and the wavelengths at which the atmosphere is most transparent do not coincide. By numerical integration of the area under the "HgCdTe" curve between limits of 8.0 and 12.5 μm , one arrives at an "SNR" of $2.44 \times 10^6 \text{ Hz}^{1/2}/\text{cm/K}$; from the area under the "InSb" curve from 3.0 to 5.3 μm , one obtains a corresponding value of $0.576 \times 10^6 \text{ Hz}^{1/2}/\text{cm/K}$. Note that introducing the particular atmosphere and path length represented by Fig. 2 has degraded the performance of the InSb detector more than the HgCdTe detector such that the advantage of HgCdTe has increased to 4.2 to 1.

According to the LOWTRAN 7 atmospheric transmission model, over paths containing large quantities of water vapor (i.e., long paths and high absolute humidities), the transparency of the atmosphere degrades with range at a greater rate in the 8- to 13- μm band than in the 3.0- to 5.3- μm band and that a crossover point exists beyond which performance in the latter band is superior [Milton et al., 1975]. However, there is a body of anecdotal and some quantitative evidence that LOWTRAN underpredicts atmospheric transmittances in the long wavelength infrared band by as much as a factor of ten [Hess, et al., 1985]. Therefore, the predicted crossover may not occur in reality.

Since SNR (Eq. 1) in a passive IR imaging device is proportional to the square root of the number of detectors, equivalent sensitivity could be achieved under the set of circumstances covered in Fig. 10 by using about 18 times (4.2^2) as many InSb detectors as HgCdTe detectors in basically the same set.

CLIMATE CONSIDERATIONS

Another consideration involved in the choice of spectral band is the climate in the region where the IR imaging sensor is expected to be used. The frigid zones are characterized by very low concentrations of water vapor in the atmosphere, by moderate to high concentrations of water in the form of small liquid or solid particles, and by a

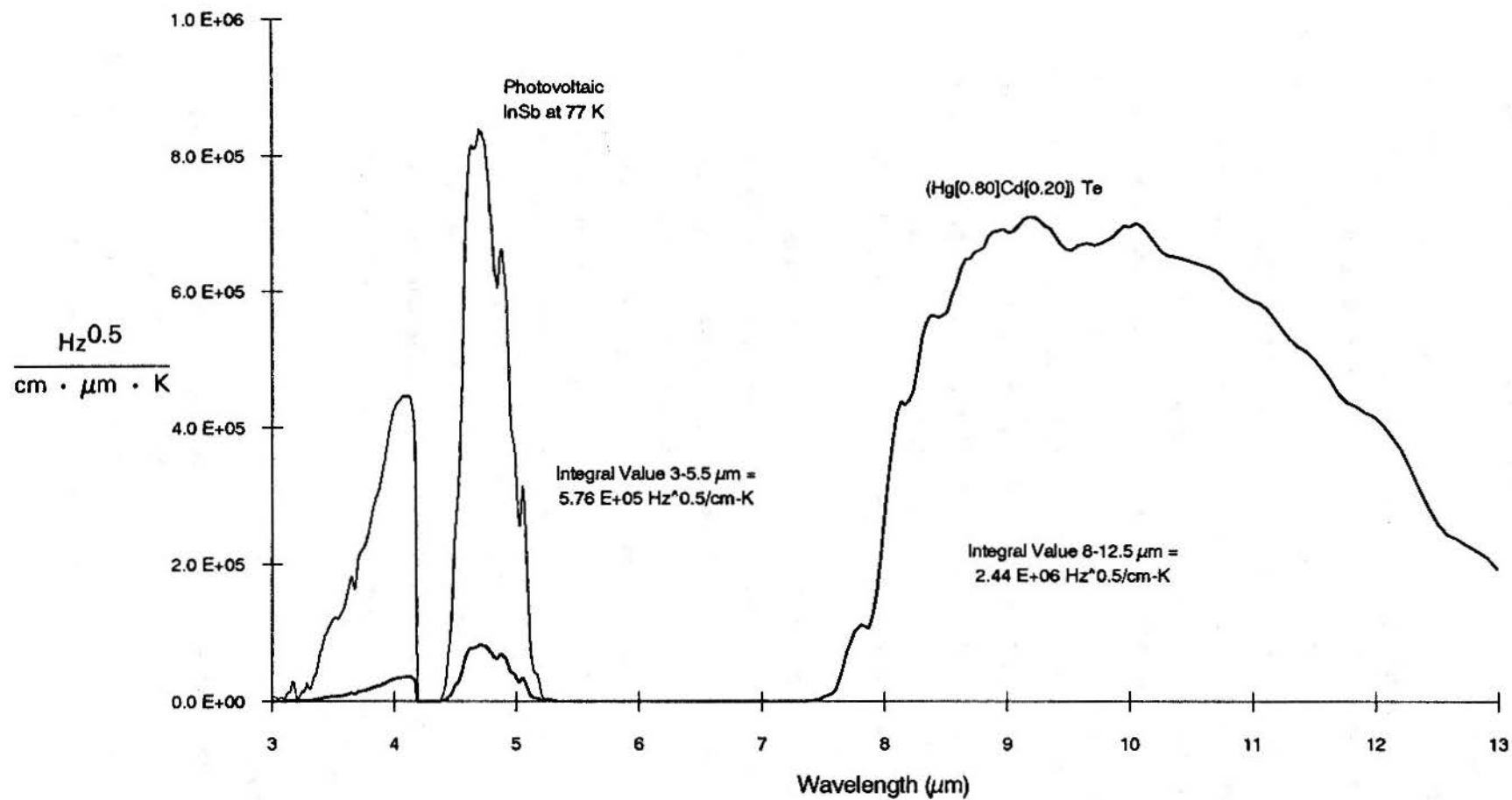


Figure 10. Spectral detectivities of selected IR detectors weighted by the thermal derivative of spectral radiance of a 288-K blackbody and the spectral transmittance of a selected atmospheric path.

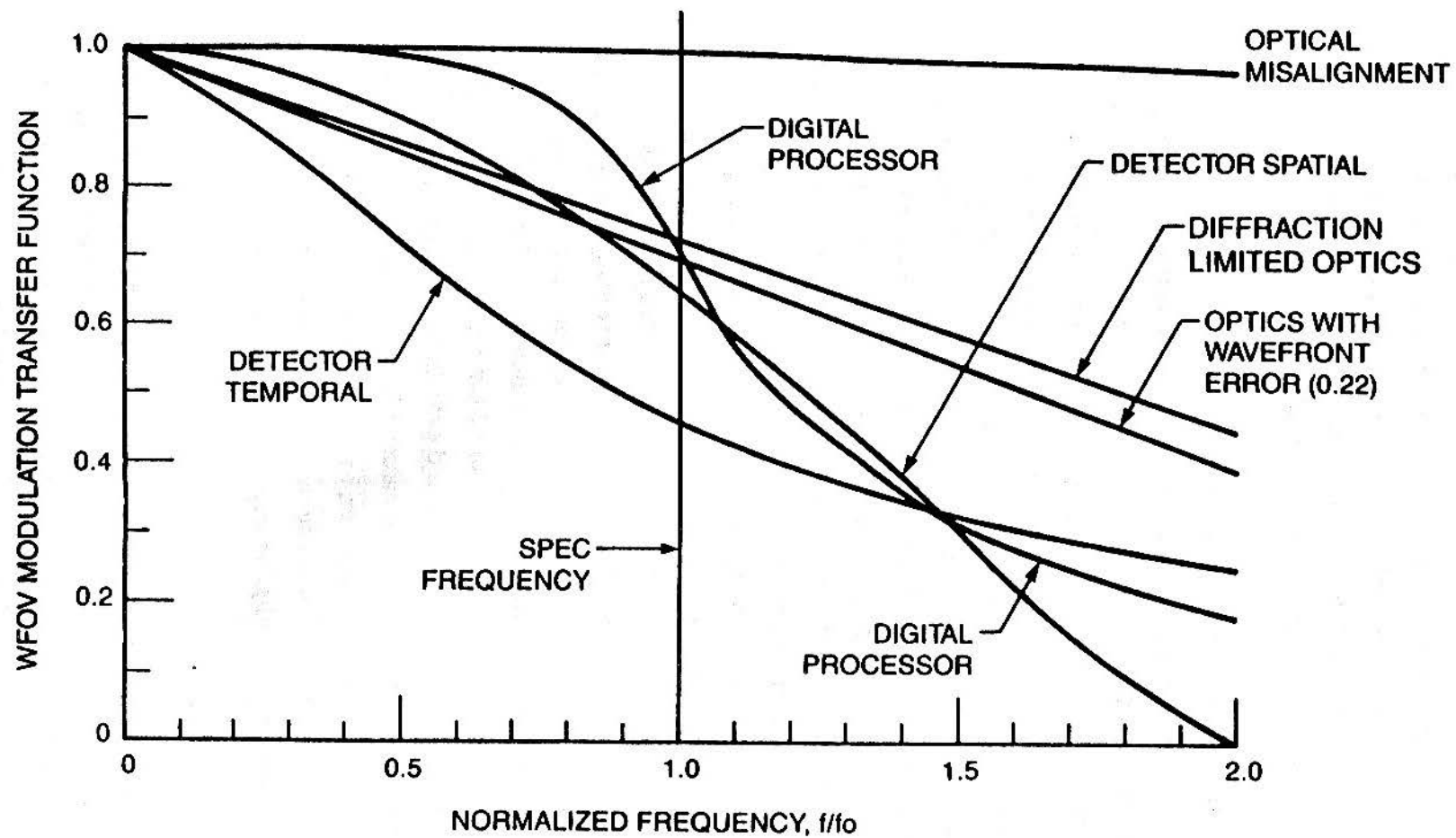
spectral distribution of radiation from targets and backgrounds shifted toward longer wavelengths because of their low temperatures. These three factors tend to favor a choice of operating in the far-IR waveband band. On the other hand, in the tropics, high absolute humidity, relatively low aerosol content in the atmosphere, and higher temperature targets and backgrounds tend to favor mid-IR equipment.

EFFECTS OF DIFFRACTION ON RESOLUTION

Another factor involved in the choice of spectral band is diffraction. In the past, when IR imaging sets employed only one or a few detectors, designs revolved about achieving adequate sensitivity by use of large optics and large detectors and only scant attention was paid to diffraction. However, as larger arrays of smaller detectors became feasible, achieving adequate sensitivity became of lesser concern and achieving higher resolution was emphasized. Ultimately, a point was reached at which angular resolution could no longer be expressed simply as the ratio of detector size to focal length but rather, in accordance with the Rayleigh criterion, as 2.44 times the ratio of wavelength to aperture diameter. Thus, as IR imaging devices operating in the far-IR waveband band evolved, resolution rather than sensitivity became the function driving IR sensor designs to larger and larger apertures. One method of circumventing this fundamental limitation is to employ the shorter wavelengths of the mid-IR waveband thereby raising the possibility of gaining (roughly) a two-fold improvement in resolution with a given aperture size. For IRLSs, however, the resolution performance is not typically limited by diffraction but by the spatial and temporal response of the detector array. Figure 11 shows the various contributions to the modulation transfer function (MTF) of the ATARS IRLS which is designed to operate with 8- to 12- μm HgCdTe detectors. If these detectors were replaced by 3- to 5.3- μm detectors and everything else kept constant, there would be an improvement (increase) in the values of the curve labeled "diffraction-limited optics" by a factor of about 2.5. However, because the system MTF (not shown) is the product of all the component MTFs, changing the spectral band (to reduce the effects of diffraction) would yield a negligible improvement in resolution.

OPTICAL MATERIALS

Still another factor in the choice of spectral band is the availability of suitable optical materials. There is a relative dearth of window and lens materials which are transparent in the 8- to 13- μm band and which exhibit other properties necessary for their use on aircraft such as hardness, mechanical strength, insolubility in water, and acceptable cost. The material which approaches these requirements most closely at



[ATARS IRLS CDR, 30 May - 2 June 1989]

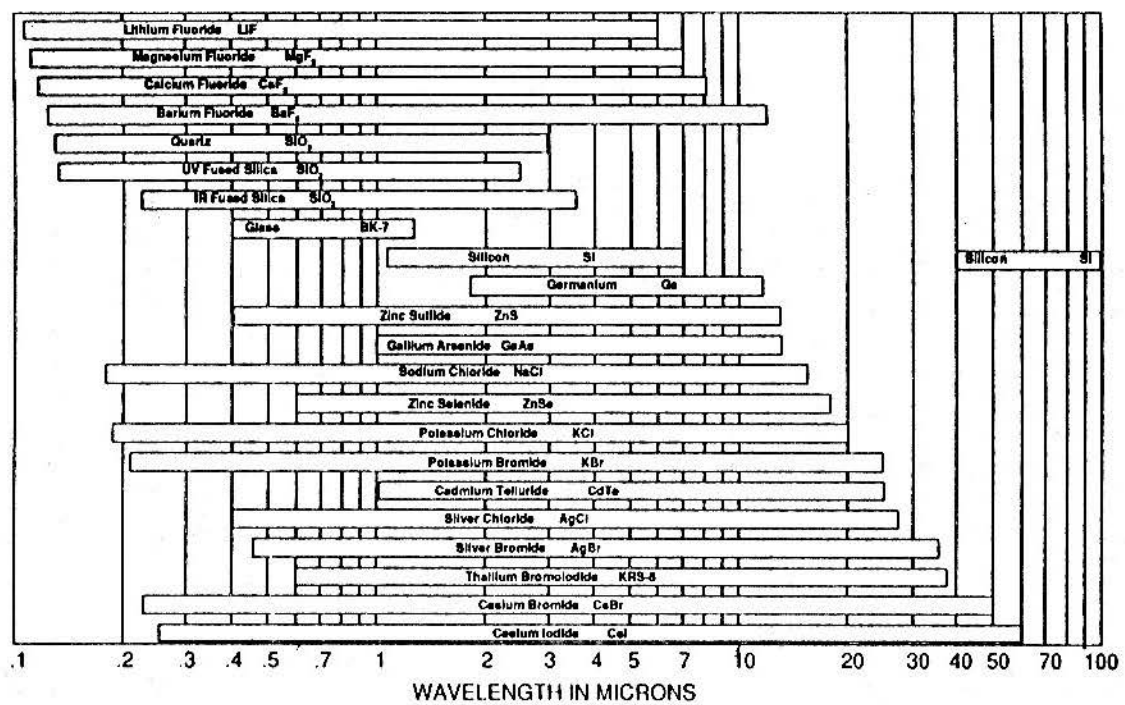
Figure 11. Contributions to the MTF of the ATARS IRLS.

present is germanium. Unfortunately, germanium is opaque over the visible waveband. Transmission bands of other common optical materials are illustrated in Fig. 12. Figure 12 shows that there are only a limited number of materials that are transmissive over both the visible (0.38 to 0.78 μm) and IR wavebands. There is a greater availability of materials that would be acceptable for operation over the mid-IR and visible bands than over the far-IR and visible bands. Calcium fluoride and magnesium fluoride are both excellent optical material candidates for mid-IR and visible operations. They both exhibit the hardness, mechanical strength, and water insolubility characteristics that are required for a tactical airborne application. There appear to be no optical materials that would be acceptable for operation over both the visible and far-IR wavebands. Most of the materials (in Fig. 12) that exhibit the required transmissive characteristics (i.e., sodium chloride, barium fluoride, potassium chloride, potassium bromide, cesium bromide, and cesium iodide) are water soluble and would not be acceptable optical materials to be exposed to normal atmospheric conditions. The most likely candidate would be zinc sulfide but its cut-on wavelength (0.5 μm) (see Fig. 13) would partially inhibit transmission of part of the visible spectrum (violet and blue). There is the possibility that the water soluble materials could be used in conjunction with a special coating (e.g., glassy diamond). The utilization of these special coatings implies a greater level of complexity, which can result in higher costs and risks.

There are also more exotic materials that were not included in Fig. 12 owing to availability and cost limitations. The best known of these exotic optical materials are diamond and sapphire. Diamond is optically transmissive from 0.25 to 80 μm , and sapphire is transmissive from 0.14 to 6.5 μm [Wolfe and Zissis, 1985].

The other optical characteristics that can affect the waveband selection are the availability of broad-band reflective optics. Figure 14 illustrates the reflective characteristics of the most commonly used reflective materials. Figure 14 shows that several common metallic reflection materials are available that can be used over the visible, mid-IR, and far-IR wavebands.

Most IRLSs utilize reflective optics and operate over an open slot in the bottom of the aircraft. They do not require a mechanical window, and the reflective optics could operate over both the IR and visible wavebands. Accordingly, availability of suitable optical materials should not be a compelling factor in the choice of waveband for a line scanner.



[JANOS Technology Inc.]

Figure 12. Transmission bands of common optical materials (10% transmission, 2 mm thickness).

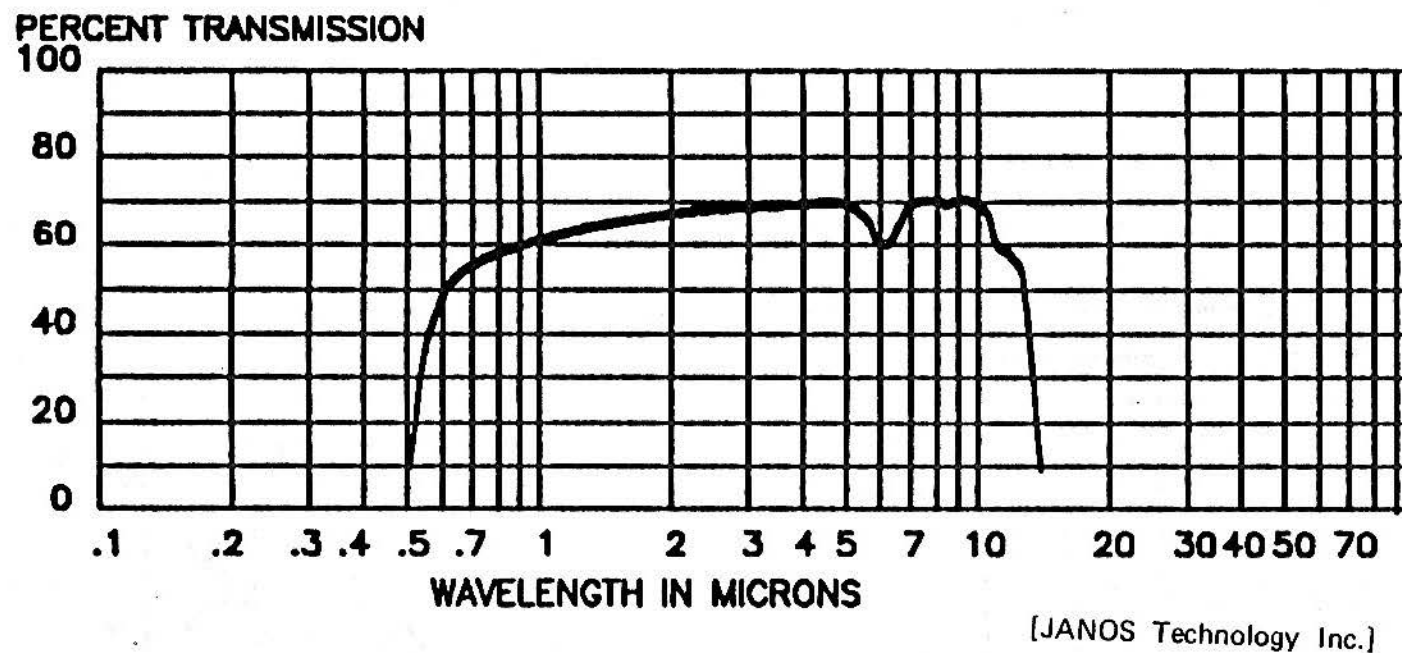


Figure 13. Optical transmission of zinc sulfide (5 mm thickness).

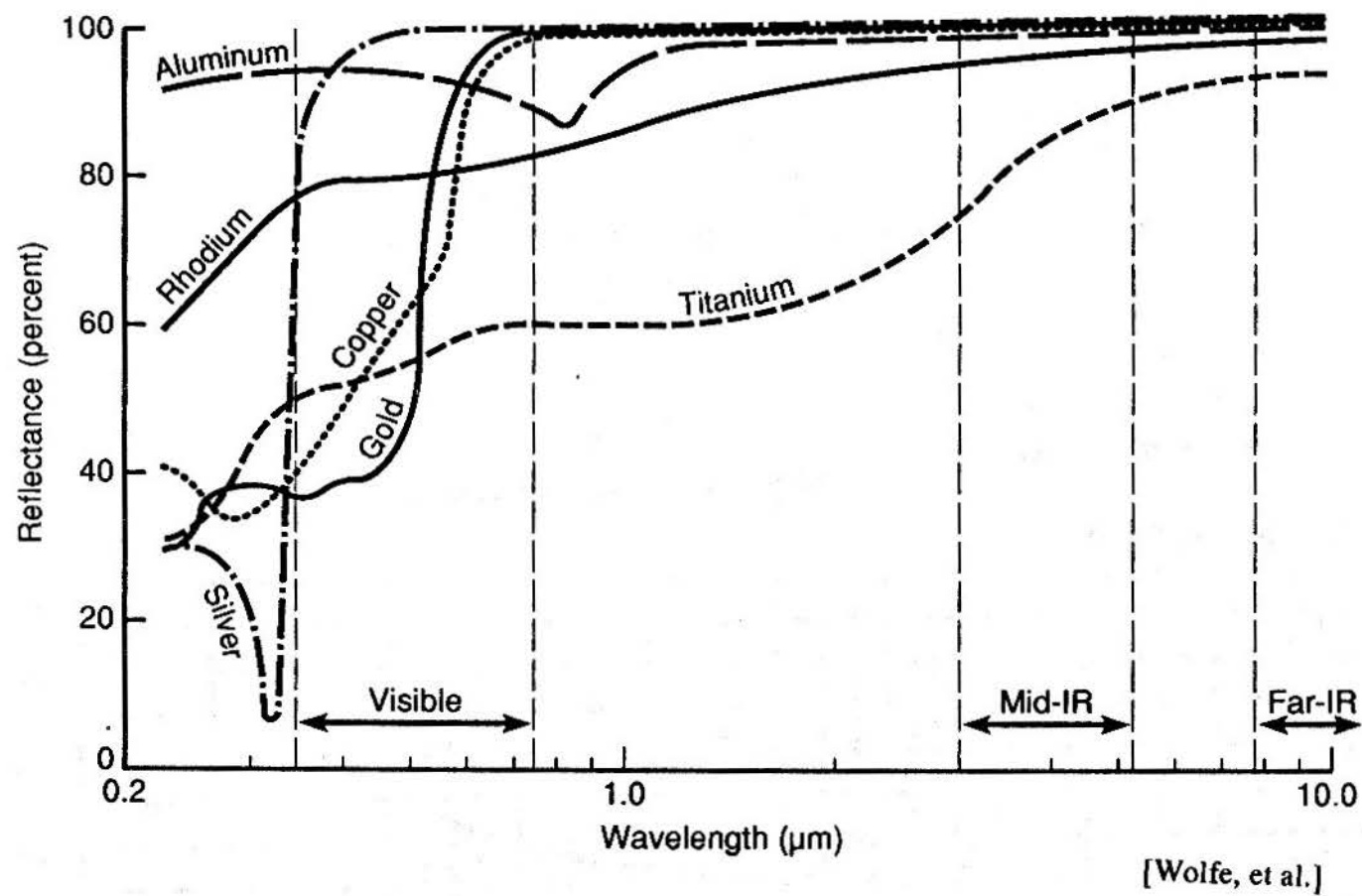


Figure 14. Reflectivities of common metallic coatings.

DETECTOR COOLING

Prior to the development of the HgCdTe detector, quantum detectors (eg., Ge:Cu, Ge:Hg) operating in the 8- to 13- μ m band required cooling to about 35 K or below, whereas 3.0- to 5.3- μ m detectors (e.g., InSb, PbSe) required cooling to about 80 K or below. The added difficulty of cooling to the lower temperature was an important consideration in the choice of spectral band. The advent of HgCdTe has alleviated the low temperature cooling requirement associated with the 8- to 13- μ m band since HgCdTe operates satisfactorily at 80 K. An additional factor is the power dissipation requirement. Photovoltaic (PV) devices exhibit minimal power dissipation. HgCdTe is available as both photoconductive (PC) and PV devices. The PC devices exhibit a much more mature technology but impose additional heat dissipation requirements. The increased power dissipation requirement for PC devices is not a driver for a line scanning sensor owing to the small number of detector elements.

The cryogenic refrigerator requirements are driven by the temperatures they must produce and the amount of power they must dissipate. Several closed cycle (Stirling) and linear nitrogen refrigerators are currently commercially available that can dissipate from 1/4 to 2 W while maintaining temperatures of 77 to 80 K. These refrigerators have been developed primarily in support of Army common module programs and can be considered off-the-shelf items that are fairly reliable. Cooling to lower temperatures (17 to 35 K) requires more complex refrigerators that are significantly larger, more costly, and less reliable.

Thermoelectric (TE) coolers could further reduce weight and volume while increasing reliability. (TE coolers have no moving parts.) Unfortunately, TE coolers cannot currently obtain sufficiently low enough temperatures. The best that has been obtained is 100 K by Marlow Industries using a ten-stage bismuth-telluride device. As the temperatures achievable with TE coolers become lower and as new detector materials are developed which can operate at higher and higher temperatures, it is conceivable that an overlap of these temperature ranges will occur and thermoelectrically cooled IR detectors suitable for use in airborne IR imaging devices will become a reality. This possibility is much more likely to occur for mid-IR detectors than for far-IR detectors and could quite conceivably precipitate renewed interest in the shorter wavelength band.

There are some 3- to 5- μ m detectors that are currently available that can be TE cooled, but they suffer other limitations. The currently available detector material PbSe can operate in the mid-IR waveband at temperatures achievable with current

thermoelectric coolers. However, because of its long time constant, it is not suitable for use at the high scanning rates employed in mechanically scanned airborne IR imaging devices of conventional design. PtSi is another mid-IR detector material that can be TE cooled, but PtSi has a low cut-off wavelength (less than 4 μm) and a relatively low quantum efficiency.

SPECTRAL BAND LIMITS

After one has decided upon which spectral band appears better, subject to the considerations discussed above, one must next consider the limits of the chosen band. If all of the radiant energy impinging on the detector comes from the target (and none, say, from the intervening atmosphere), then the broadest band possible would be the optimum. This situation would be approximated by an IR imaging device viewing a target at very short ranges such as in a laboratory. If the set employs an HgCdTe detector, it would operate best without filtering over a broad band, say, from about 2 to 15 μm . If, however, radiation from other sources, such as the atmosphere and the various optical elements in the IR sensor itself, impinges on the detector, the SNR yielded by such a broadbanded system will not be the optimum achievable. To illustrate, in those spectral intervals (e.g., 5.4 to 7.5 μm) where the atmosphere is quite opaque over representative ranges, not only does the atmosphere absorb information-bearing radiation from the target before it can get to the sensor but it also replaces it with an amount of its own self-emitted radiation consistent with its own temperature. This non-information-bearing radiation from the atmosphere impinges on the detector in the form of an unsteady stream of photons whose degree of unsteadiness is proportional to the square root of the number of photons arriving. This unsteadiness in the photon flow generates noise in the detector which reduces the ratio of target signal to system noise. Thus, it is desirable to exclude spectrally by use of filters that radiation which would otherwise degrade the performance of the set. One can arrive at an optimum band, for any given set of conditions, by first calculating the system SNR for some small spectral interval (such as from 9.0 to 10.0 μm) and then repeating the calculation for a succession of incrementally larger intervals until further increases begin to show a decrease in SNR [Barhydt et al., 1970]. Of course, the limits of the optimum band will depend upon the characteristics of the prevailing atmosphere and the path length through it. Therefore, the choice of spectral band limits for an airborne IR imaging device will always be a matter of compromise.

COMPLEMENTARITY VERSUS REDUNDANCY OF IMAGED TARGET INFORMATION

If a dual spectrum system is to be developed that produces imagery in the visible part of the spectrum and in one IR band (either long-IR or mid-IR), some additional considerations apply. To get the maximum useful information from a dual spectrum imaging device there should be substantial differences in the character of the imagery in one band compared with the other. That is, when both bands are being used simultaneously, the resulting information should be complementary rather than redundant. For example, the visible radiation band would be used to sense light reflected off objects in the scene whereas an IR band would be used to sense radiation emitted by them. Although there should be sufficient similarity in the imagery in the two bands to permit association (even registration) of one with the other (mostly shape information), there should be sufficient differences to warrant use of a second band; that is, there should be enough additional information provided to make a second band worth while. Figure 15 illustrates how the character of the imagery varies depending upon the selection of wave band, for one particular set of daytime conditions. The curve on the left represents the spectral distribution of reflected solar radiation and the curve on the right represents emitted radiation. A sensor operating in the visible light band responds primarily to reflectivity variations in the scene whereas one operating in the far-IR (8 to 13 μm) IR band responds primarily to temperature variations in the scene. The mid-IR (3 to 5.3 μm) IR band, however, straddles both curves and responds about equally to reflected solar radiation and to temperature-related emitted radiation. Thus, there is a certain ambiguity in daytime mid-wavelength IR imagery. To illustrate, suppose it is necessary to distinguish between asphalt and concrete paving material on an airfield. Because asphalt is black, it will absorb most of the solar radiation impinging on it and increase to a higher temperature than the concrete. It will therefore appear relatively "hot" in the far-IR band but relatively dark in the visible band because it reflects little. In the mid-IR band, it is not clear a priori whether the asphalt will appear brighter or darker than the concrete; indeed, the two might appear equally bright if the incremental radiation reflected from the concrete equals the incremental radiation emitted from the asphalt.

COMPARISON OF REFLECTED AND EMITTED RADIATION FROM A GRAYBODY

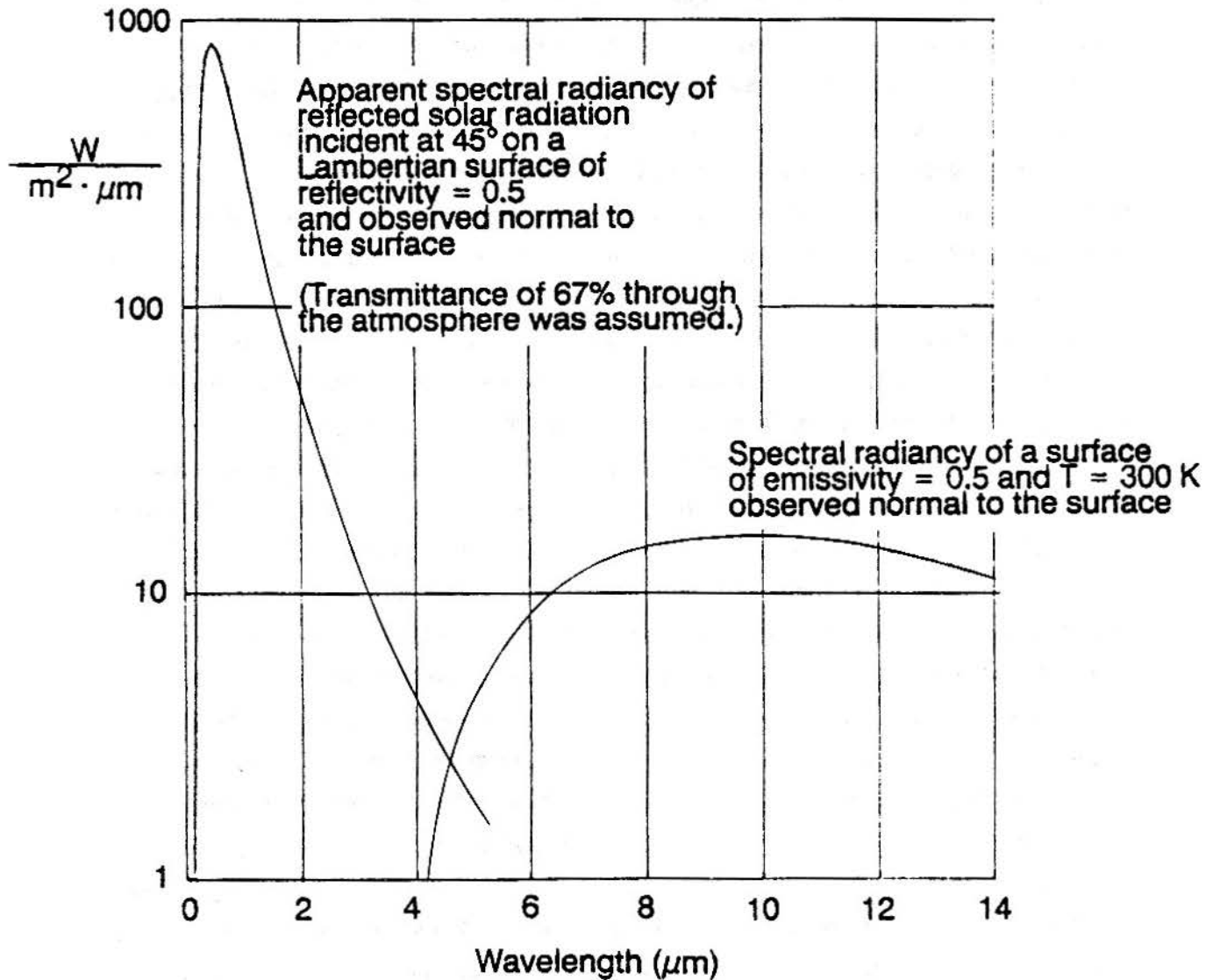


Figure 15. Comparison of reflected and emitted radiation from a graybody.

IMAGING THROUGH AEROSOL DISTRIBUTIONS

If conditions are such that one band (e.g., the visible band) is essentially shut down because of haze, smoke screens, battlefield dust or camouflage, the other band (e.g., the IR band) could fill the gap. In general, the longer the wavelength of the radiation used by the sensor relative to the size of the particulates suspended in the atmosphere, the better the transmission through the scattering medium. For the far-IR band, the wavelength is about 20 times greater than for visible light, whereas for the mid-IR band the wavelength is only about 8 times greater than for visible light.

SECTION 3

CONCLUSIONS

Although detectors operating in the mid-IR band exhibit values of peak detectivity D^* that are about 5 times greater than those of far-IR detectors, the factor of 21 greater amount of radiant power available from room-temperature scenes in the long-wavelength band relative to the mid-wavelength band is a compelling reason to choose the former. The fact that the technology of mid-wavelength detectors is more mature and that such detectors can be built into large arrays is not a convincing argument for selecting an inferior band. Although contrasts (expressed in terms of percent change in radiated power per degree change in target temperature) are greater in the mid-wavelength band, this apparent advantage is illusory (except for staring systems) because one is dealing simply with a larger percentage of a much smaller number. Percent contrast is not a significant factor in a.c.-coupled systems such as IR line scanners.

The arguments based on the use of the LOWTRAN model for selecting the mid-IR band over the far-IR band for long-range imaging through clear atmospheres of high absolute humidity are not valid for the line scanner situation being considered here because long transmission paths (e.g., tens of miles) are not typically encountered with line scanners.

Diffraction effects are not significant factors because, in line scanners, resolution is governed largely by the detector and not by diffraction and because wavelength-indifferent reflective optics are the general rule. The choice of optical material is not a significant factor as long as a reflective optical design is employed and the equipment operates through an aerodynamic window.

Choosing the far-IR waveband for the IR portion of a dual spectrum IR/visible light imaging system provides a greater degree of complementarity and a lesser amount of redundancy than choosing the mid-IR waveband.

It is concluded that the optimum wavelength band for the IR channel of a dual spectrum line scanner is the far-IR waveband (8 to 13 μm).

REFERENCES

- Moser, P. M., and N. E. MacMeekin, *Index of Performance for FLIR (Forward Looking Infrared) Imaging Devices*, NAVAIRDEVCON Report No. NADC-72167-AE, 10 Apr 1973 (AD-525116).
- Milton, A. F., G. L. Harvey, J. C. Kershenstein, and M. D. Mikolosko, *Comparison of the 3-5-Micrometer and 8-12-Micrometer Regions for Advanced Thermal Imaging Systems Using the LOWTRAN II Atmospheric Transmission Model*, NRL Memorandum Report 3098, Aug 1975.
- Hess, M. R., J. Gibbons, J. Toner, W. Abrams, R. Chin, M. Gibbons, and M. Winn, *The Long Focal Length Imaging Demonstration (LFLID) Project*, Proc. IRIS Imaging, 1985.
- JANOS Technology Inc., *Precision Optics and Components*, 1989.
- Wolfe, W. L. and G. J. Zissis, *The Infrared Handbook, Revised Edition*, 1985.
- Barhydt, H., D. P. Brown, and W. B. Dorr, *Comparison of Spectral Regions for Thermal-Imaging Infrared Sensors*, Proc. IRIS, Vol. 14, No. 2, August 1970.